Statistical properties of stimulated Brillouin scattering in single-mode optical fibers above threshold

Andrei A. Fotiadi,* Roman Kiyan, Olivier Deparis, Patrice Mégret, and Michel Blondel

Faculté Polytechnique de Mons, Service d'Electromagnétisme et de Télécommunications, 31 Boulevard Dolez, B-7000 Mons, Belgium

Received June 21, 2001

We performed numerical simulations to obtain statistical and spectral characteristics of stimulated Brillouin scattering (SBS) initiated by Gaussian noise in single-mode optical fibers. Recently published experimental spectra of SBS power [e.g., Phys. Rev. Lett. **85,** 1879 (2000)] are explained completely by a one-dimensional SBS model. We give a clear physical insight into the problem and, for what is to our knowledge the first time, reveal how the probability function of Stokes power, the power-correlation function, and the SBS spectra evolve as key parameters of the model vary, leading to a modification of Stokes field statistics. © 2002 Optical Society of America

OCIS codes: 290.5900, 190.4370, 060.4370, 030.6600.

Stimulated Brillouin scattering (SBS) in optical fibers, a nonlinear process initiated by spontaneous scattering of a pump wave on occasional hypersound waves caused by thermal noise, exhibits complicated dynamic behavior[1–12] that can be employed in applications.

Stochastic properties of SBS in fibers are usually described in terms of spectral and statistical functions.[13] In previous studies both the Stokes field and the power-related functions have been used for this purpose. For example, the studies reported in Refs. 2–4 concentrated on determination of the Stokes field spectrum, $S(\nu)$, including direct measurements of Brillouin linewidth, $\Delta\nu_S$,[3,4] where $S(\nu) = \mathcal{F}\{B(\tau)\}$ is defined as the Fourier transform of the correlation function of the Stokes amplitude, $B(\tau) = \langle E_S(t)E_S{}^*(t+\tau)\rangle/\langle E_S(t)E_S{}^*(t)\rangle$. However, the experiments reported in Refs. 5 and 6 were devoted to recording the temporal behavior of the Stokes power, $P_S(t)$, and yielded a spectrum of Stokes power, $S_P(\nu)$, that was essentially $S_P(\nu) = \langle|\mathcal{F}\{P_S(t)\}|\rangle \equiv \mathcal{F}\{C(\tau)\}^{1/2}$, where $C(\tau) = \langle P_S(t+\tau)P_S(t)\rangle/\langle P_S(t)\rangle^2 - 1$ is the power-correlation function. In the high-gain limit[3] below the SBS threshold, both spectra, i.e., $S(\nu)$ and $S_P(\nu)$, have a Gaussian line shape and both narrow in a similar manner as the pump power is increased. Above threshold, spectrum $S(\nu)$ saturates to a Gaussian shape with a fixed linewidth.[3] Concerning spectrum $S_P(\nu)$, experimental results were recently reported[6] that show that the spectrum above threshold becomes inhomogeneous, exhibiting strong broadening and characteristic hole burning as the pump power is increased. This phenomenon is referred to by the authors of Ref. 6 as a feature of a three-dimensional interaction between the pump and the Stokes waves in a fiber waveguide.

Remaining within the frame of the one-dimensional SBS model (i.e., completely ignoring the three-dimensional dynamics of SBS interaction), we have carried out numerical simulations to reproduce the experimental data reported in Ref. 6. We demonstrate in this Letter that the specific features of Stokes power spectrum $S_P(\nu)$ and power-correlation function $C(\tau)$, which was reported in early experiments,[3,7] are both closely connected with a modification of the Stokes field statistics above threshold. Until now, the statistics of the Stokes field has been studied only for SBS below and near threshold and was found to be a Gaussian stochastic process with zero mean.[8] Here the statistical properties of SBS above threshold are presented for what is to our knowledge the first time. Specifically, we reveal how the probability function of the Stokes power, $W(P_S)$, the power-correlation function, $C(\tau)$, and both SBS spectra, $S(\nu)$ and $S_P(\nu)$, evolve as key parameters of a one-dimensional SBS model vary, leading to a modification of the Stokes field statistics.

Simulations are based on the following equations for complex amplitudes of pump wave $E_L(z, t)$, Stokes wave $E_S(z, t)$, and hypersound wave $\rho(z, t)$ (Refs. 3, 4, and 9):

$$\begin{aligned}
\frac{n}{c}\frac{\partial E_L}{\partial t} + \frac{\partial E_L}{\partial z} &= -\frac{g}{2S}\rho E_S,\\
\frac{n}{c}\frac{\partial E_S}{\partial t} - \frac{\partial E_S}{\partial z} &= \frac{g}{2S}\rho^* E_L,\\
T_2\frac{\partial \rho}{\partial t} + \rho &= E_L E_S{}^* + f(z,t),
\end{aligned} \tag{1}$$

where g is the SBS gain factor, T_2 is the hypersound relaxation time, S is the effective mode area, c is the velocity of light in vacuum, n is the refractive index, and z is the coordinate along the fiber. The complex amplitudes $E_L(z, t)$ and $E_S(z, t)$ are normalized such that $E_L E_L{}^* = P_L$ and $E_S E_S{}^* = P_S$, where P_L and P_S are the pump and the Stokes powers, respectively. The Langevin noise source, $f(z, t)$, is a spatially and temporally δ-correlated Gaussian random process with zero mean: $\langle f(z', t')f^*(z'', t'')\rangle = Q\delta(z' - z'')\delta(t' - t'')$. In our calculations, noise intensity $Q = 320\sqrt{5\pi}\chi_a S^2 \exp(-20)/(g^2 L_a T_2)$ was chosen so that the pump-power–Stokes-power conversion efficiency was equal to $\chi_a = 1\%$ at pump-power level $P_a = 20S/(gL_a)$ for a fiber length $L_a = 200$ m. The boundary conditions corresponded to the injection of a monochromatic cw pump wave at $z = 0$, i.e., $E_L(0, t) = \sqrt{P_0}$, $E_S(L, t) = 0$. The other parameters in the calculations are related to SBS in typical telecommunication fiber at pump wavelength $\lambda_L \approx 1$ μm: $g = 2.5 \times 10^{-9}$ cm/W, $T_2 = 10$ ns, and $S = 25$ μm^2 (note that $T_2 \sim {\lambda_L}^2$ and $g \sim T_2/{\lambda_L}^2$).[10]

0146-9592/02/020083-03$15.00/0

For any given fiber length L, the threshold power level is referred to as $P_{\text{th}} = 20S/gL$.[1] Two dimensionless parameters, $N = P_0/P_{\text{th}} = T_0/10T_1$ and $\gamma = T_1/T_2$, that determine the Stokes-wave dynamics are defined as the ratio of key temporal parameters of the SBS process: the time that light takes to travel through the fiber, $T_0 = nL/c$; the time associated with the effective SBS amplification length, $T_1 = 2nS/cgP_0$; and the hypersound decay time, T_2. Numerical integration of Eqs. (1) based the fourth-order Runge–Kutta algorithm, with temporal step $h_t \approx \min\{T_0, T_1, T_2\}/10$, was performed for a wide range of parameters: $N = 1$–10 and $\gamma = 0.01$–10. For a given pair $\{N, \gamma\}$, we calculated 20 different stationary realizations of Stokes field time series $E_S(0, t)$, each with a duration of 20 μs. Then, we processed these data to build functions $W(P_S)$, $B(\tau)$, $C(\tau)$, and $S_P(\nu)$, averaged over realizations. The results of the simulations are presented in Figs. 1–5.

Parameter N (pump-power level P_0 in units of times above threshold) determines the degree of pump depletion that is due to power conversion from a pump to a Stokes wave. The conversion efficiency, $\chi = \langle P_S(0, t)\rangle/P_0$, grows logarithmically with N, as shown in Fig. 1(a). As shown in Fig. 1(b), a Stokes wave generated near threshold ($N \approx 1$) exhibits large stochastic power fluctuations with power deviation, $\Delta \equiv C(0) \approx 60$–$100\%$. The pump depletion leads to specific feedback that is caused by energy exchange between the counterpropagating pump and Stokes waves. This feedback suppresses Stokes power fluctuations. At a given value $N > 1$, the suppression is determined by the parameter γ. For $\gamma \ll 1$, fluctuations are quickly inhibited as pump depletion grows, whereas for $\gamma \gg 1$ fluctuations remain large even under high pump–Stokes conversion efficiency. Figures 1(c) and 1(d) show qualitatively different behaviors of Stokes power calculated for $N = 10$ ($\chi \approx 87\%$) in two limit cases: $\gamma = 10$ ($\Delta \approx 70\%$) and $\gamma = 0.01$ ($\Delta \approx 0.4\%$), respectively.

Simultaneously with the suppression of Stokes power fluctuations, the SBS statistics is modified above threshold. The Stokes power probability function, $W(P_S/\langle P_S\rangle)$, is shown in Fig. 2, with N and γ as parameters. At any value of γ near threshold, the probability function (e.g., $N = 1.25$; curves 1) is approximately coincident with the exponential power distribution function, $W(P_S/\langle P_S\rangle) = \exp(-P_S/\langle P_S\rangle)$, which is equivalent to a Gaussian statistical distribution with zero mean for the Stokes field. Above threshold, the statistics of the Stokes field remains Gaussian only for $\gamma \gg 1$ [e.g., $\gamma = 10$; see Fig. 2(a)]. However, when $\gamma < 1$, the probability function is significantly modified above threshold [Figs. 2(b)–2(d)]. Specifically, it exhibits a maximum near $P_S/\langle P_S\rangle \approx 1$. The width of the probability function is reduced as N grows. At lower values of γ, the probability function is more densely concentrated near $P_S/\langle P_S\rangle \approx 1$.

We verified numerically that the drastic modification of SBS statistics shown in Fig. 2 does not affect the Stokes field correlation function, $B(\tau)$, and the Stokes field spectrum, $S(\nu)$. For any pair $\{N, \gamma\}$, both $B(\tau)$ and $S(\nu)$ were found to be Gaussian, with correlation time $\tau_c \approx 85$ ns and full spectrum width $\Delta\nu_B \approx 7.5$ MHz, respectively (widths at $1/e$ maximum). The variations of τ_c and $\Delta\nu_B$ were less than $\pm 10\%$ over all $\{N, \gamma\}$. This result is in quite good agreement with experiments[3,4] and theoretical estimation $\Delta\nu_B \approx (\sqrt{20}\pi T_2)^{-1}$.[2]

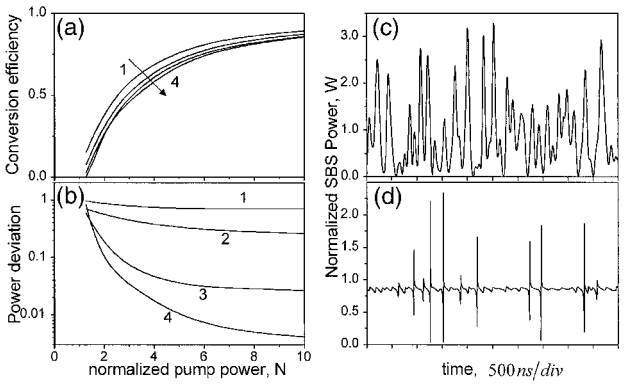

Fig. 1. (a) Pump–Stokes conversion efficiency χ and (b) Stokes power deviation Δ as functions of N for (curves 1–4) $\gamma = 10, 1, 0.1, 0.01$. Typical temporal behaviors of the Stokes power, $P_S(0, t)/P_0$, are also shown for two limit cases at $N = 10$: (c) $\gamma = 10$, (d) $\gamma = 0.01$.

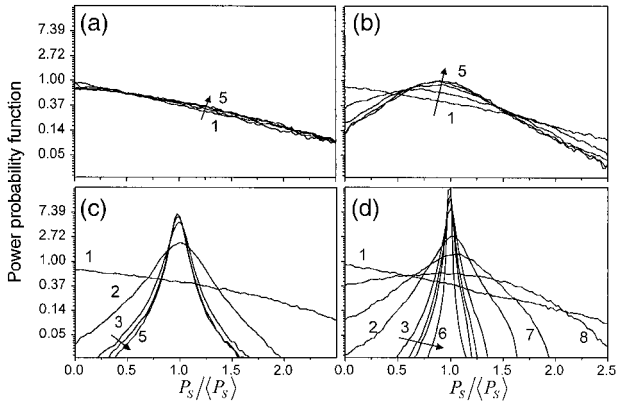

Fig. 2. Probability functions of the Stokes power for (a) $\gamma = 10$, (b) $\gamma = 1$, (c) $\gamma = 0.1$, and (d) $\gamma = 0.01$. Curves 1–8: $N = 1.25, 2.5, 5, 7.5, 10, 100, 1.9, 1.5$.

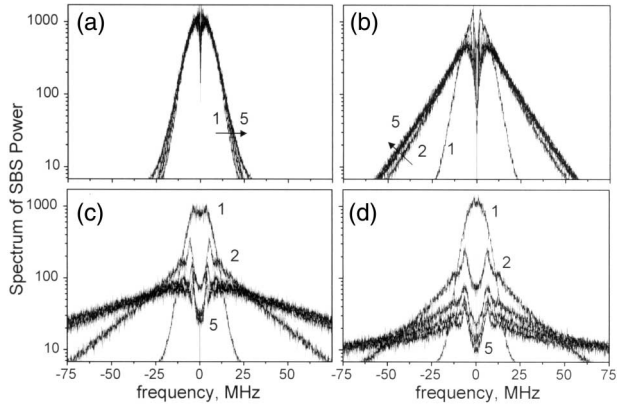

Fig. 3. Spectra of the Stokes power (normalized to average power) for (a) $\gamma = 10$, (b) $\gamma = 1$, (c) $\gamma = 0.1$, and (d) $\gamma = 0.01$. Curves 1–5: $N = 1.25, 2.5, 5, 7.5, 10$.

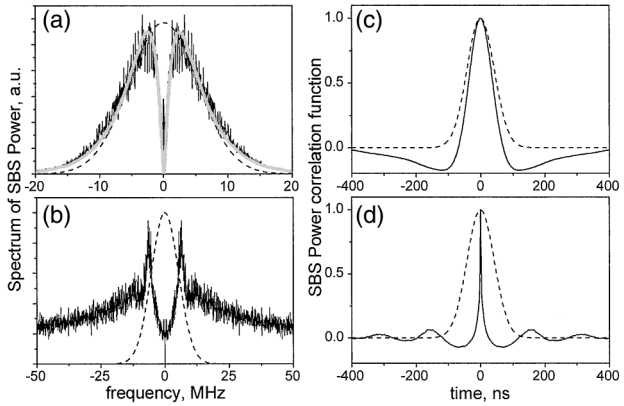

Fig. 4. Spectra $S_P(\nu)$ and correlation functions $C(\tau)/C(0)$ for (a), (c) $\gamma = 10$ and (b), (d) 0.01 and $N = 10$. Solid curves, calculated from Eqs. (1); dashed curves, evaluated for Gaussian stochastic processes with the same field spectra $S(\nu)$ as those of the processes under consideration; gray curve, $S_P(\nu) \approx K(\nu)S_P{}^{\text{th}}(\nu)$, from a linearized SBS model.[1]

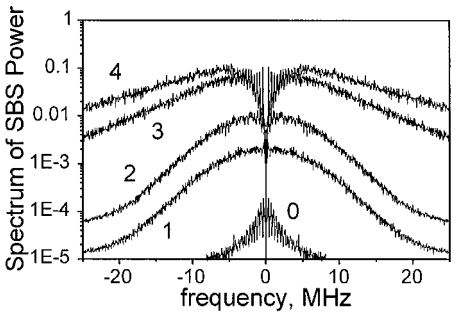

Fig. 5. Spectra of the Stokes power calculated for comparison with those from Ref. 6. The fiber length is $L = 250$ m. Curves 1–4: $N = 1.1, 1.5, 5.4, 10$; $\gamma = nL/(10cT_2N) \approx 12.5/N$. Curve 0, difference between the spectra at $N = 1.5$ and $N = 10$.

Nevertheless, the modification of the Stokes field statistics does affect the spectrum of Stokes power, $S_P(\nu)$, as shown in Fig. 3. At any value of γ near threshold ($N = 1.25$) or at $\gamma = 10$ above it, when the SBS statistics remains nearly Gaussian, the shape of the spectrum, $S_P(\nu)$, is Gaussian, with ~15-MHz width at $1/e$ maximum, which is exactly twice the width of the Brillouin line, $\Delta\nu_B$. The obvious relation between $S_P(\nu)$ and $S(\nu)$ in this case is a direct consequence of the Gaussian statistics of the SBS field, which provides a simple relation between field- and power-correlation functions, i.e., $B(\tau) = \sqrt{C(\tau)}$.[13] Modification of the SBS statistics caused either by a decrease in γ at a given $N > 1.25$ or by an increase in N at a given $\gamma < 10$ leads to broadening of the spectrum, $S_P(\nu)$, with modification of its wings. Besides, a dip appears and grows in the center of the spectrum. At moderate values of N, the width of the dip depends slightly on N and reaches ~13 MHz at $\gamma = 0.01$.

The spectrum, $S_P(\nu)$, displays features similar to those reported for the gain spectrum, $K(\nu)$, of a saturated SBS amplifier.[1,11,12] Specific features of both spectra have the same origin as $S_P(\nu)$. Indeed, Fig. 4(a) shows that $S_P(\nu)$ is well approximated by $S_P(\nu) \approx K(\nu)S_P{}^{\text{th}}(\nu)$,[1] where $S_P{}^{\text{th}}(\nu)$ is the SBS spectrum near threshold and an expression for $K(\nu)$ is given by Ref. 11. The correlation functions shown in Fig. 4 exhibit related features similar to those reported in previous experiments.[3,7]

To justify the conclusion that the one-dimensional model is able to explain experimental results, we performed calculations for the experimental conditions reported in Ref. 6. Very good agreement between the experimental[6] and the calculated spectra $S_p(\nu)$ shown in Fig. 5 was obtained.

In conclusion, we have numerically investigated SBS statistics in single-mode fiber above threshold. The main spectral and statistical functions were calculated for a wide range of parameters. We have demonstrated that hole burning and spectral broadening of the spectrum of SBS power observed in experiments[6] are well described by a one-dimensional SBS model. However, a certain dissonance still remains. The authors of Ref. 6 claimed that this phenomenon is "independent of the fiber length." According to our results, shown in Fig. 3, this is not the case.

This research was supported by Interuniversity Attraction Pole program (IAP IV 07) of the Belgian Government and the Russian Fund of Basic Research (grant N 00-02-16903). A. A. Fotiadi's e-mail address is fotiadi@telecom.fpms.ac.be.

*Also with Ioffe Physico-Technical Institute of the Russian Academy of Sciences, 194021 Politekhnicheskaya 26, St. Petersburg, Russia.

References

1. E. A. Kuzin, M. P. Petrov, and A. A. Fotiadi, in *Optical Phase Conjugation*, M. Gower and D. Proch, eds. (Springer-Verlag, Berlin, 1994), pp. 74–96.
2. R. W. Boyd, K. Rzazewski, and P. Narum, Phys. Rev. A **42,** 5514–5521 (1990).
3. A. L. Gaeta and R. W. Boyd, Phys. Rev. A **44,** 3205–3209 (1991).
4. A. A. Fotiadi and R. V. Kiyan, Opt. Lett. **23,** 1805–1807 (1998).
5. R. G. Harrison, J. S. Uppal, A. Johnstone, and J. V. Moloney, Phys. Rev. Lett. **65,** 167–170 (1990).
6. V. I. Kovalev and R. G. Harrison, Phys. Rev. Lett. **85,** 1879–1882 (2000).
7. A. A. Fotiadi and E. A. Kuzin, in *Quantum Electronics and Laser Science Conference*, Vol. 16 of 1995 OSA Technical Digest Series (Optical Society of America, Washington, D.C., 1995), pp. 128–129.
8. E. M. Dianov, A. Ya. Karasik, A. V. Luchnikov, and A. K. Senatorov, Sov. J. Quantum Electron. **19,** 508–512 (1989).
9. E. M. Dianov, A. Ya. Karasik, A. V. Luchnikov, and A. N. Pilipetskii, Opt. Quantum Electron. **21,** 381–395 (1989).
10. G. P. Agrawal, *Nonlinear Fiber Optics*, 2nd ed. (Academic, Boston, Mass., 1995).
11. A. A. Fotiadi, E. A. Kuzin, M. P. Petrov, and A. A. Ganichev, Sov. Techn. Phys. Lett. **15,** 434–436 (1989).
12. Y. Takushima and K. Kikuchi, Opt. Lett. **20,** 34–36 (1995).
13. L. Mandel and E. Wolf, *Optical Coherence and Quantum Optics* (Cambridge U. Press, Cambridge, 1995).